AIAA AVIATION Forum
June 15-19, 2020, VIRTUAL EVENT
AIAA AVIATION 2020 FORUM

10.2514/6.2020-3289

Effect of Active Feather Length on Aerodynamic Performance of Airfoils at Low Reynolds Number Flow

Ali Esmaeili[1] and Masoud Darbandi[2]
Sharif University of Technology, P.O. Box 11365-11155, Tehran, Iran

Gerry E. Schneider[3]
University of Waterloo, Waterloo, Ontario, N2L 3G1, Canada

To increase the flight endurance of a Micro air vehicle (MAVs), which operates at low Reynolds number flow, one way is to harvest energy during its flight. By inspiring from the nature when all the birds use their feathers to control and distribute their power along the flying time, a solution might be design of a piezoelectric plate as feathers, which scavenges energy directly from the fluid flow. Cantilevered beam with piezo-ceramic layer undergoing vortex-induced vibrations can convert the mechanical energy available from the ambient environment to a usable electrical power. Since a flow-driven piezoelectric composite beam takes a form of natural three-way coupling of the turbulent fluid flow, electrical circuit and structural behavior of the beam, the difficulties of modeling and simulations would be sharply increased. Also there are a lot of parameters, which effect on the performance of active feather such as its length. Therefore, effect of its length are studied and several feathers with different lengths are numerically examined.

I. Nomenclature

b	=	width of piezoelectric beam
L	=	length of piezoelectric beam
f	=	fluid force
$f_p(x.t)$	=	the net pressure forces acting on the surface of the beam
$f_v(x.t)$	=	the net viscous forces acting on the surface of the beam.
c	=	an arbitrary constant depending on the initial condition
ω_{rd}	=	damped natural frequency of the rth mode.
$\phi_r(x)$	=	mass normalized of the beam for the rth mode
$\eta_r(t)$	=	modal coordinate of the beam for the rth mode
x	=	along the beam axis
y	=	absolute displacement of the beam in the transverse direction (i.e., in y-direction)
t	=	time
$v(t)$	=	output voltage
Y_p	=	piezoelectric elasticity modulus
Y_s	=	substrate elasticity modulus
e_{31}	=	piezoelectric coupling coefficient
ρ_p	=	piezoelectric density
ρ_s	=	substrate density

[1] Postdoctoral Fellow, Department of Aerospace Engineering.
[2] Professor, Department of Aerospace Engineering, Center of Excellence in Aerospace Systems.
[3] Professor, Department of Mechanical and Mechatronics Engineering, AIAA Associate Fellow.

h_p = piezoelectric thickness
h_s = substrate thickness
ε_{33}^S = permittivity

II. Introduction

Limitations in the available volume and energy sources during the operations of fixed wing micro aerial vehicles (MAVs) are the dominant reasons of their weaknesses such as low flight time and endurance. To further increase the time duration of flight, it is necessary to find ways to higher the airframe endurance. An excellent biological example for efficient flight time is the flight of Alaskan bar-tailed godwit who can fly eight-day, 11000 km autumn migration from Alaska to New Zealand in one step, with no stopovers to rest or refuel. The important features for extreme endurance are the capability of the bird to carry a fuel load and a well-streamlined body shape, which helps to reduce the drag created by the body. The observation of the godwit wing shows the existence of a range of feathers length along the trailing edge of wing which can inspired by the aerodynamicists to increase the flight endurance of small air vehicles.

On the other hand, scavenging usable electrical energy during the MAV's fight can resuscitate the power discharges or at least provide the power required for the auxiliary equipment such as actuators and sensors. The availability of additional energy sources becomes even more important as the utilization of heavier batteries to power auxiliary systems further reduces the payload capacity of an MAV. During their flight, MAVs are subjected to structural nonlinearities and unsteady aerodynamic forces, which give rise to aeroelastic vibrations [1][2]. The transformation of these into a usable form of energy has been the subject of many studies in the field of Aerospace [3] and others. A wide variety of transduction mechanisms has been proposed for that purpose, namely piezoelectric, electromagnetic and electrostatic [4][5]. Consequently due to claimed advantages such as high power density, architectural simplicity and scalability, piezoceramic composite elements have established themselves as the preferred choice for the majority of the researchers in the field [6][7][8]. Recently, the flow-induced movements are one of the most potential energy sources and can be converted to a usable energy in various flow conditions by utilizing energy harvesters. The literature includes investigations of energy harvesting from the flapping of piezoelectric films [9][10][11][12]and cantilever beams located behind bluff bodies [13][14][15]. The interaction between an upstream aerofoil-based energy harvester and a downstream harvester has been experimentally studied with the aim of determining the flow features impacting on the harvester located downstream. The results have showed that the wake of the windward harvester had significant effects on the vibration amplitude, frequency, and power output of the trailing devices [16]. A rectangular wing-based EH system with a piezoelectric generator attached has been designed and experimentally tested [17]. It is demonstrated that the aeroelastic rolling frequency increased with the generator attached, whereas the rolling amplitude decreased. To study the effects of the free-play nonlinearity on the performance of an aerofoil-based energy harvester, a rigid airfoil mounted vertically has been experimentally investigated and illustrated that by increasing the free-play nonlinearity gap, the cut-in speed has been reduced through a subcritical instability and energy could be harvested at low wind speeds [18]. However, reports of experimental testing in real or simulated flight conditions are very scarcely found in the literature and more proofs of concept are instrumental to advance this technology. As an alternative option, design and assessment of different aspects of the energy harvester properties can only be provided by the numerical simulation.

In the present study, a piezoelectric cantilever beam which is mounted at the trailing edge of an airfoil is numerically studied. The beam operates like an active feathers and converts the flow induced vibration to the electrical energy. Moreover, effect of feather length on the amount of harvested energy and aerodynamic performance are investigated. To simulate the active beam, an aero-electro-mechanical coupling method is applied so that an exact electromechanical solution of a cantilevered piezoelectric energy harvester based on energy method and Euler-Bernoulli beam theory is coupled to the fluid flow equations (Navier-Stokes equations).

III. Modelling, Equations and Numerical Methods

In this research, a unimorph harvester which consists of a uniform composite Euler–Bernoulli beam made of a polyvinylidene fluoride (PVDF) layer perfectly bonded to the substructure layer is considered. The harvester is connected to the electrical circuit through the electrodes, which bracket the PVDF layer. It is also assumed that the harvester is excited persistently by the fluid flow, thus continuous electrical outputs can be drawn from the resistive load. Furthermore, the leakage resistance of the PVDF is negligible in the electrical circuit and the capacitance of the active layer is considered as internal to the PVDF rather than showing it as an external element parallel to the resistive

load, and the piezoelectric constitutive relations generate the electrical capacitance term. Therefore, the capacitance of the piezoelectric layer is not ignored and it is considered in the circuit equation.

A simplification into a topology of discrete entities approximating the behavior of the spatially distributed system is applied when lumped parameter models are used [19][20]. However, accurate predictions require distributed parameters modeling, directly or indirectly involving the Rayleigh-Ritz method and the extended Hamilton's principle (along with energy considerations) to derive the governing equations [21][22]. Analytical solutions with closed-form expressions can be obtained in the foregoing case by assuming appropriate eigenfunctions [23].

The harvester beam is typically excited by the fluid force exerted by a passing vortex. Additionally, two types of damping mechanisms will be included: viscous air (medium) damping and Kelvin–Voigt (or strain-rate) damping. Hence, the mechanical equation of motion with electrical coupling in the absolute x–y frame can be achieved as follow:

$$YI\frac{\partial^4 y(x.t)}{\partial x^4}+c_s I\frac{\partial^5 y(x.t)}{\partial x^4\partial t}+c_a\frac{\partial y(x.t)}{\partial t}+m\frac{\partial^2 y(x.t)}{\partial t^2}+\vartheta v(t)\left[\frac{d\delta(x)}{dx}-\frac{d\delta(x-L)}{dx}\right]=F(t) \tag{1}$$

In order to solve these electromechanical coupling equations, the beam transversal displacement $y(x.t)$ can be expressed by absolutely and uniformly convergent series of the eigenfunctions based on the expansion theorem, i.e.:

$$\mathrm{y(x.t)}=\sum_{r=1}^{\infty}\phi_r(x)\eta_r(t) \tag{2}$$

Now, the relative displacement of the beam introduced by Eq. (2) can be substituted into the electromechanical equations (Eq. (1)). By considering orthogonality conditions of the eigenfunctions [24] and using Eq. (2) in Eq. (1), the electromechanically coupled ordinary differential equation may be obtained and the solution of this equation can be extracted using the Duhamel integral [25]:

$$\eta_r(t)=\frac{1}{\omega_{rd}}\int_{\tau=0}^{t}[f(t)-\chi_r v(\tau)]e^{-\zeta_r\omega_r(t-\tau)}\sin\big(\omega_{rd}(t-\tau)\big)\,d\tau. \qquad \chi_r=\vartheta\left.\frac{d\phi_r(x)}{dx}\right|_{x=L} \tag{3}$$

where $\omega_{rd}=\sqrt{1-\zeta_r^2}$ is the damped natural frequency of the r[th] mode. In summary, final solution is expressed for voltage across the electrical as follow:

$$v(t)=e^{-t/\tau_c}\left(\int e^{t/\tau_c}\sum_{r=1}^{\infty}\varphi_r\frac{d\eta_r(t)}{dt}dt+c\right) \tag{4}$$

where

$$\varphi_r=-\frac{d_{31}Y_p h_{pc}h_p}{\varepsilon_{33}^S L}\int_{x=0}^{L}\frac{d^2\phi_r(x)}{dx^2}dx=-\left.\frac{d_{31}Y_p h_{pc}h_p}{\varepsilon_{33}^S L}\frac{d\phi_r(x)}{dx}\right|_{x=L} \tag{5}$$

Since zero initial displacement and zero initial velocity of the beam are assumed, the arbitrary constant is zero (c=0).

Next, the coupled electromechanical equations, Eq. (3) and Eq. (4), are obtained such that the output voltage ($v(t)$) and mechanical responses ($\eta_r(t)$) are found by solving those equations. Subsequently, the transversal displacement of the beam at each position can be determined from the mechanical response in Eq. (2).

From fluid flow governing equations, the viscous and incompressible flow are described by the unsteady Navier-Stokes equations. In the (unsteady) Reynolds-Averaged Navier-Stokes (RANS) turbulence modeling, the non-turbulent unsteadiness is resolved in the mean flow via finite-time ensemble averaging, whereas a closure model is used to describe the turbulent fluctuations. Among the plethora of available choices, the transitional SST k-ω turbulence model (Wilcox, 2006) has been chosen for the current investigation because of its superior performance in the prediction of flows in the presence of adverse pressure gradients. This model comprises additional transport equations for the turbulent quantities k and ω, and makes use of an eddy viscosity (Esmaeili et al., 2018). The interaction of the transition model with the SST turbulence model takes place via modification of the original terms as production and destruction of turbulent kinetic energy, using an 'effective' intermittency that also takes into account separation-induced transition. For a more comprehensive description of all the steps and definitions in this modeling approach, denoted in the present study by T-RANS, the reader is referred again to Ref. (Langtry and Menter, 2009).

Here, the aforementioned equations are solved by the finite volume method, which is based on a discretization of integral forms of the conservation equations. Based on the control volume formulation of analytic fluid dynamics, the solution domain is initially divided into a finite number of discrete volumes or cells, where all variables are stored at

their geometric centers. The equations are then integrated over all the control volumes by utilizing the Gaussian theorem, and the result of the integration combines cell-face convection and diffusion fluxes. The diffusion flux is approximated by central differences and the discretization of the convective flux is determined by the QUICK (Quadratic Upwind Interpolation for Convective Kinematics) scheme.

A. Coupling Algorithm

Scavenging electrical power from flexible piezoelectric cantilever beams excited by the surrounding fluid involves the mutual interaction of the air flow (aerodynamics), the mechanical structure and the electrical circuit, thus requiring a three-way coupling algorithm. The fluid flow exerts a distributed force on the harvester's surfaces and deforms the structure, inducing mechanical strains within the piezoelectric layers. An electrical charge is generated in the piezoelectric layer due to the cyclic mechanical strain, and the charge is provided to the harvester circuit. The response of the circuit feeds back into the piezoelectric structure, influencing the structural response and finally modifying the fluid flow field. All of these interactions can be modeled by the governing equations of each sub-field with the addition of the appropriate coupling terms. Fig. 1 shows the flowchart of the algorithm achieving a consistent system coupling.

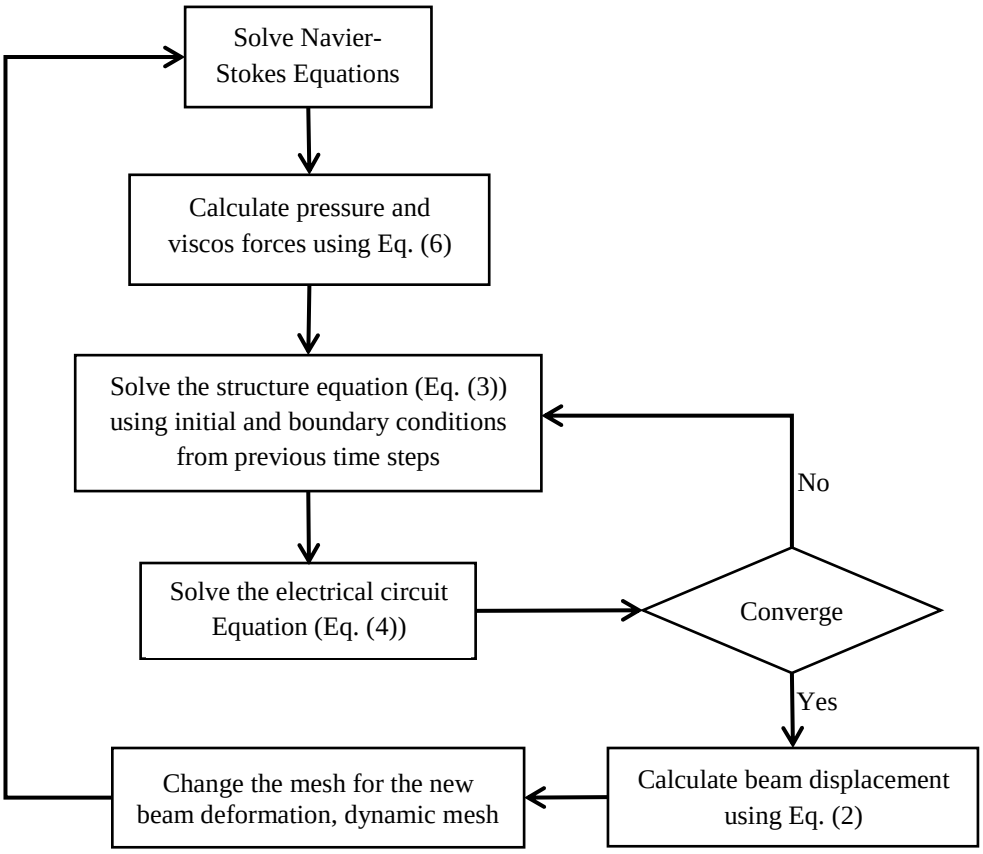

Fig. 1 Numerical procedure of the aero-electro-mechanics coupling algorithm in each time step.

The force induced by the fluid flow is obtained from the pressure distribution and wall viscous shear stress by integration over the surface of the piezoelectric beam. The spatially distributed fluid force in each mesh cell is projected onto the mass normalized eigenfunctions, as follows:

$$f(t) = \int_{x=0}^{L} (f_p(x.t) + f_v(x.t))\phi_r(x)dx \tag{6}$$

In each time step, the fluid-induced modal force (f) is assumed constant and used in the solution of the structure equation.

The electromechanical coupled equations, Eqs. (3) and (4), are solved iteratively until the converged voltage and the mechanical response are found. The beam deflection is measured using Eq. (2), and the fluid mesh is subsequently changed accordingly. Finally, the RANS equations are solved on the deformed fluid domain (computational grid), and the corrected forces on the beam surfaces are measured. These solution steps are repeated in each time step until the changes in the deformation of the beam have converged.

B. Solution Domain and material properties

An airfoil (infinite wing) with cross section of NASA LS (1)-0417, and a chord length of 232 mm, is considered here in a more applied study for piezoelectric energy harvesting. The free-stream velocity is 8.81 m/s, which corresponds to a constant Reynolds number of 140,000, and the turbulence level in the free-stream is prescribed at approximately 1%. Therefore, a fully turbulent vortex street may be expected to be formed at this Reynolds number, which is suitable to extract energy from it.

In addition, a unimorph harvester consisting of one layer of piezoelectric material PVDF and a layer of Mylar is installed at the trailing edge of the airfoil in different configurations. Figure 2 shows the airfoil, and the energy harvester mounted as a flapping flag. The physical properties of this piezoelectric beam are given in Table (1).

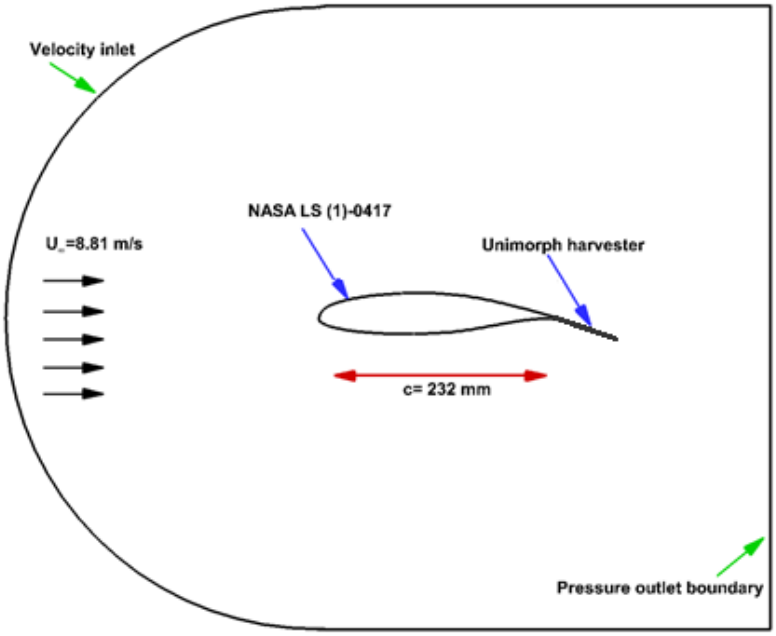

Fig. 2 Schematic of a unimorph piezoelectric beam mounted as a flapping flag at the trailing edge of a NASA LS (1)-0417 airfoil.

IV. Results and Discussion

Aiming to design the energy harvester for generating power from the flow-induced vibrations, the vortex shedding frequency must be quantified first. However, the interaction between the piezoelectric beam characteristics and vortex shedding parameters is a key point to get maximum harvesting power. Concerning the presence of the piezoelectric cantilever beam, the maximum electrical power conversion is normally to occur when the harvester beam fluctuates at its first natural frequency. But when a piezoelectric beam will be added to the trailing edge of an airfoil and can be moved due to aerodynamic forces the vortex shedding properties would be changed. As seen in the nature, the birds' feather length plays an important role on their maneuverability and performances; therefore, the length of active beam can be a vital parameter for the mentioned interaction.

Table 1. Physical properties of the piezoelectric cantilever beam.

Piezoelectric (PVDF) properties	
Elasticity modulus	$Y_p = 3\ GPa$
Piezoelectric coupling coefficient	$e_{31} = 0.07\ C/m^2$
Density	$\rho_p = 1780\ Kg/m^3$
Piezoelectric thickness	$h_p = 28\ \mu m$
Length	L=30 mm
Width	b=16 mm
Permittivity	$\varepsilon_{33}^S = 0.08\ nF/m$
Mylar (substrate) layer properties	
Elasticity modulus	$Y_s = 3.79\ GPa$
Layer thickness	$h_s = 172\ \mu m$
Density	$\rho_s = 1390\ Kg/m^3$

Initially, the time evolution of the instantaneous vertical velocity component (Y-velocity) at a point close to the trailing edge of airfoil is measured and the shedding frequency is found to be 9.2 Hz when there is not the beam. It is noteworthy that the computed frequency of vortex shedding from of two-dimensional airfoil is remarkably close to that of the corresponding finite wing. A minor effect of the aspect ratio was also noted earlier for rectangular wings in the Reynolds number range of $10^4 - 10^5$ [26]. In the current study, the Strouhal number based on the cross-stream length scale of the airfoil ($\omega c\ sin(\alpha)/U_\infty$) is calculated, and its value is 0.22, which is in good agreement with the value (0.2) presented in a previous experimental study [26]. However, the presence of a splitter plate mounted at the trailing edge of the airfoil influence the vortex shedding from the airfoil, and these effects depend on the location of the plates and its length. Hence, different beam lengths are chosen as 6.5, 13, 19.5 and 25 percents of the airfoil chord. To have a comparison between aerodynamic forces, Table (2) illustrates the aerodynamic coefficients of airfoil with splitter plate by various lengths. As seen here, there is an optimum length to generate maximum lift coefficient but drag coefficient has a linear trend with the plate length and always decreases by increasing the active length. The lift-to-drag ratio (L/D) is also compared in Fig. 3, which confirms existence of an optimum length for the active plate aerodynamically.

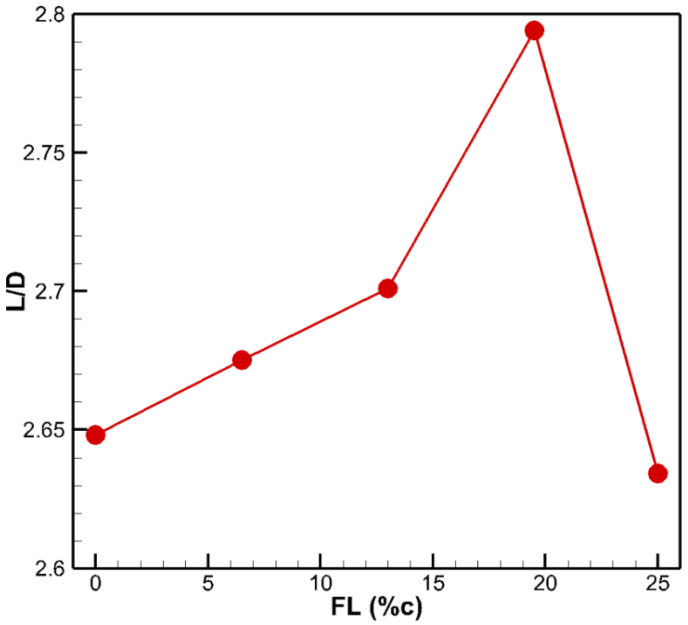

Fig. 3 Comparison of lift-to-drag ratio of the airfoil with different feather length at α = 14 deg.

Table 2. Comparison of aerodynamic coefficients of airfoil with various feather lengths at angles of attack of 14 degrees.

Feather length FL (% of chord)	Cl	Cd
0	1.52	0.574
6.5	1.26	0.471
13	1.31	0.485
19.5	1.33	0.476
25	1.03	0.391

The pressure coefficient distribution on the piezoelectric beam is also compared in Figure 4. As the figure shows, the pressure difference between the top and bottom surfaces of the beam are increasing by the longer plate and as a result of this, the lift coefficient grows. However, increasing the length of plate can improve the pressure loss at the trailing edge but this length is very critical and if it is very small, the flow on the bottom surface of airfoil can rotate to top surface but by increasing the length, the flow cannot move from bottom to top surface of airfoil. It is noteworthy that if this length would be longer than the required one, the vortex on the top surface of airfoil can grow bigger and finally the lift-to-drag ratio drops sharply.

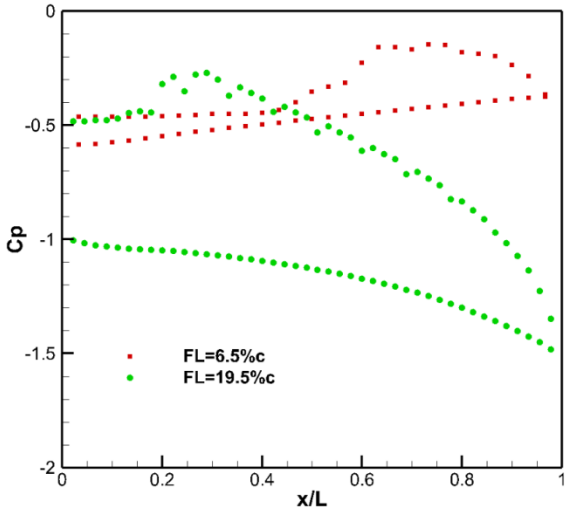

Fig. 4 Pressure coefficent distribution on the piezoelectric beam surfaces for two different dimensionless lengths at α = 14 deg.

The flow field around the airfoil with and without active feather is demonstrated in Fig. 5. The results illustrate that the lift and drag coefficients increase 5.7% and 1.5%, respectively when the active feathers are allowing to move by the flow field. Also, the piezoelectric layer could convert around one miliwatt energy from the vortex shedding.

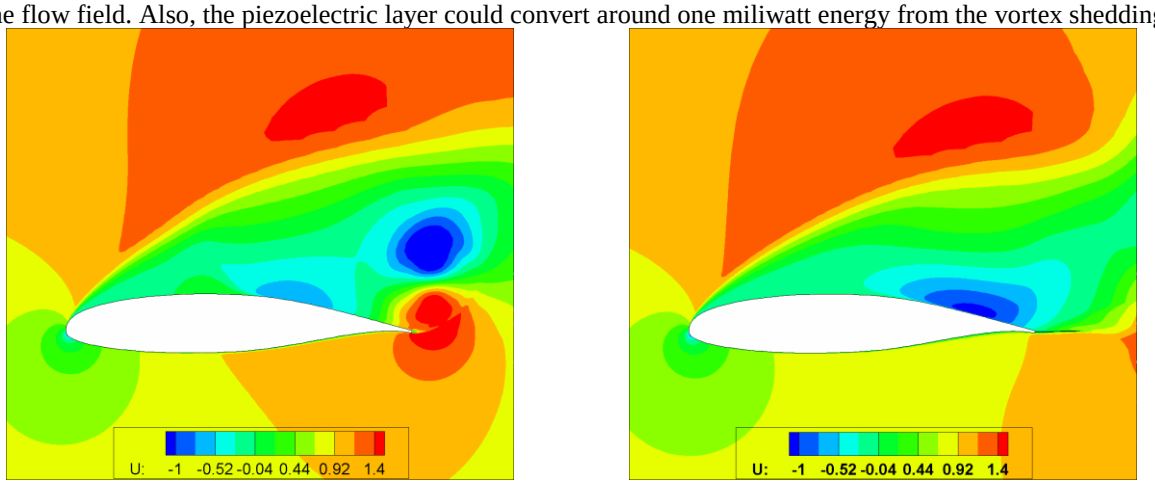

(a) **(b)**

Fig. 5 Comparison of (in-plane) instantanious chordwise velosity over (a) the base airfoil and (b) the airfoil in the presence of active feather (with electrical resistance of 1000 Ω) at α = 20 deg.

V. Conclusions

In this paper, investigation of the flow-driven cantilevered piezoelectric harvesters was considered to scavenge electrical energy from the turbulent wake flow formed on the top surface of an infinite wing. The fluid flow passing around the wing carries a lot of energies, which can be converted to the electrical power. The force induced on the surface of harvester comes from the vortex shedding emanating from the leading edge of the airfoil and triple coupling algorithm is also applied to communicate between the multi physics such as the fluid dynamic, structure and electrical equations. Hence, a three-way coupling algorithm was applied, so that the equations governing the fluid dynamics, structural and electrical components were coupled adequately. The fluid flow force was obtained by solving the Navier-Stokes equations and the transitional k-ω SST turbulence model. Furthermore, a distributed parameter electromechanical model was derived for the piezoelectric plate, giving rise to an analytical formulation based on the Euler-Bernoulli beam assumptions. Aiming to simulate a flow-driven piezoelectric beam, the distributed electromechanical model was modified to combine with the fluid flow equations, and the so-called aero-electro-mechanical model was obtained. The results obtained with this procedure were compared with the previously published data, showing a good agreement with them.

References

[1] Xiang, J., Wu, Y., and Li, D. "Energy Harvesting from the Discrete Gust Response of a Piezoaeroelastic Wing: Modeling and Performance Evaluation." *Journal of Sound and Vibration*, Vol. 343, 2015, pp. 176–193. https://doi.org/10.1016/J.JSV.2014.12.023.

[2] Tam Nguyen, H.-D., Pham, H.-T., and Wang, D.-A. "A Miniature Pneumatic Energy Generator Using Kármán Vortex Street." *Journal of Wind Engineering and Industrial Aerodynamics*, Vol. 116, 2013, pp. 40–48. https://doi.org/10.1016/J.JWEIA.2013.03.002.

[3] Li, D., Wu, Y., Da Ronch, A., and Xiang, J. "Energy Harvesting by Means of Flow-Induced Vibrations on Aerospace Vehicles." *Progress in Aerospace Sciences*, Vol. 86, 2016, pp. 28–62. https://doi.org/10.1016/J.PAEROSCI.2016.08.001.

[4] Boisseau, S., Despesse, G., and Seddik, B. A. *Electrostatic Conversion for Vibration Energy Harvesting*. InTech, 2012.

[5] Wei, C., and Jing, X. "A Comprehensive Review on Vibration Energy Harvesting: Modelling and Realization." *Renewable and Sustainable Energy Reviews*, Vol. 74, 2017, pp. 1–18. https://doi.org/10.1016/J.RSER.2017.01.073.

[6] Toprak, A., and Tigli, O. "Piezoelectric Energy Harvesting: State-of-the-Art and Challenges." *Applied Physics Reviews*, Vol. 1, No. 3, 2014, p. 031104. https://doi.org/10.1063/1.4896166.

[7] Roundy, S., and Wright, P. K. "A Piezoelectric Vibration Based Generator for Wireless Electronics." *Smart Materials and Structures*, Vol. 13, No. 5, 2004, pp. 1131–1142.

[8] Esmaeili, A., and Sousa, J. M. M. "Power Density Ratio Optimization of Bimorph Piezocomposite Energy Harvesters Using a Multidisciplinary Design Feasible Method." *Composite Structures*, Vol. 165, 2017, pp. 171–179. https://doi.org/10.1016/J.COMPSTRUCT.2017.01.031.

[9] Djavareshkian, M. H., Esmaeli, A., and Parsani, A. "Aerodynamics of Smart Flap under Ground Effect." *Aerospace Science and Technology*, Vol. 15, No. 8, 2011, pp. 642–652. https://doi.org/10.1016/j.ast.2011.01.005.

[10] Djavareshkian, M. H., Esmaeili, A., Parsania, A., and Ziaforoughi, A. "3D Investigation on the Aerodynamic of Smart Flap for WIG Vehicle." *Transactions of the Japan Society for Aeronautical and Space Sciences Journal*, Vol. 9, 2011. https://doi.org/10.2322/tastj.9.51.

[11] Michelin, S., and Doare, O. "Energy Harvesting Efficiency of Piezoelectric Flags in Axial Flows." *Journal of Fluid Mechnics*, 2012. https://doi.org/10.1017/jfm.2012.494.

[12] McCarthy, J. M., Watkins, S., Deivasigamani, A., John, S. J., and Coman, F. "An Investigation of Fluttering Piezoelectric Energy Harvesters in Off-Axis and Turbulent Flows." *Journal of Wind Engineering and Industrial Aerodynamics*, Vol. 136, 2015, pp. 101–113. https://doi.org/10.1016/J.JWEIA.2014.10.021.

[13] Amini, Y., Emdad, H., and Farid, M. "Piezoelectric Energy Harvesting from Vertical Piezoelectric Beams in the Horizontal Fluid Flows." *Scientia Iranica*, Vol. 24, No. 5, 2017, pp. 2396–2405. https://doi.org/10.24200/sci.2017.4240.

[14] Akaydin, H. D., Elvin, N., and Andreopoulos, Y. "Energy Harvesting from Highly Unsteady Fluid Flows Using

Piezoelectric Materials." *Journal of Intelligent Material Systems and Structures*, Vol. 21, No. 13, 2010, pp. 1263–1278. https://doi.org/10.1177/1045389X10366317.

[15] Akaydın, H., Elvin, N., and Andreopoulos, Y. "Wake of a Cylinder: A Paradigm for Energy Harvesting with Piezoelectric Materials." *Experiments in Fluids*, Vol. 49, No. 4, 2010, pp. 291–304.

[16] Bryant, M., Mahtani, R. L., and Garcia, E. "Wake Synergies Enhance Performance in Aeroelastic Vibration Energy Harvesting." *Journal of Intelligent Material Systems and Structures*, Vol. 23, No. 10, 2012, pp. 1131–1141. https://doi.org/10.1177/1045389X12443599.

[17] Zhao, D., and Ega, E. "Energy Harvesting from Self-Sustained Aeroelastic Limit Cycle Oscillations of Rectangular Wings." *Applied Physics Letters*, Vol. 105, No. 10, 2014, p. 103903. https://doi.org/10.1063/1.4895457.

[18] Abdelkefi, A., and Hajj, M. R. "Performance Enhancement of Wing-Based Piezoaeroelastic Energy Harvesting through Freeplay Nonlinearity." *Theoretical and Applied Mechanics Letters*, Vol. 3, No. 4, 2013. https://doi.org/10.1063/2.1304101.

[19] Roundy, S., Wright, P., and Rabaey, J. "A Study of Low Level Vibrations as a Power Source for Wireless Sensor Nodes." *Computer communications*, Vol. 26, No. 11, 2003, pp. 1131–1144. https://doi.org/10.1016/S0140-3664(02)00248-7.

[20] Dutoit, N., Wardle, B., and Kim, S. "Design Considerations for MEMS-Scale Piezoelectric Mechanical Vibration Energy Harvesters." *Integrated Ferroelectrics*, Vol. 71, No. 1, 2005, pp. 121–160.

[21] DuToit, N., and Wardle, B. "Experimental Verification of Models for Microfabricated Piezoelectric Vibration Energy Harvesters." *AIAA journal*, Vol. 45, No. 5, 2007, pp. 1126–1137. https://doi.org/10.2514/1.25047.

[22] Elvin, N. G., and Elvin, A. A. "A General Equivalent Circuit Model for Piezoelectric Generators." *Journal of Intelligent Material Systems and Structures*, Vol. 20, No. 1, 2009, pp. 3–9. https://doi.org/10.1177/1045389X08089957.

[23] Erturk, A., and Inman, D. J. "An Experimentally Validated Bimorph Cantilever Model for Piezoelectric Energy Harvesting from Base Excitations." *Smart Materials and Structures*, Vol. 18, No. 2, 2009, p. 025009(18pp). https://doi.org/10.1088/0964-1726/18/2/025009.

[24] Erturk, A., and Inman, D. J. "On Mechanical Modeling of Cantilevered Piezoelectric Vibration Energy Harvesters." *Journal of Intelligent Material Systems and Structures*, Vol. 19, No. 11, 2008, pp. 1311–1325. https://doi.org/10.1177/1045389X07085639.

[25] Erturk, A., and Inman, D. J. "A Distributed Parameter Electromechanical Model for Cantilevered Piezoelectric Energy Harvesters." *Journal of Vibration and Acoustics*, Vol. 130, No. 4, 2008, p. 041002. https://doi.org/10.1115/1.2890402.

[26] Rojratsirikul, P., Genc, M. S., Wang, Z., and Gursul, I. "Flow-Induced Vibrations of Low Aspect Ratio Rectangular Membrane Wings." *Journal of Fluids and Structures*, Vol. 27, No. 8, 2011, pp. 1296–1309. https://doi.org/10.1016/J.JFLUIDSTRUCTS.2011.06.007.